ELSEVIER

Phase diagram of O/Ru(0 0 0 1) from first principles

J.-S. McEwen [a,*,1], S.H. Payne [a], C. Stampfl [b]

[a] *Department of Physics and Atmospheric Science, Dalhousie University, Halifax, Nova Scotia, Canada B3H 3J5*
[b] *Fritz-Haber-Institut der Max-Plank-Gesellschaft, Faradayweg 4-6, D-14195 Berlin-Dahlem, Germany*

Received 16 April 2002; in final form 10 June 2002

Abstract

The lattice gas model with hcp and fcc sites is used to study the O/Ru(0 0 0 1) adsorbate system. With interactions obtained from density functional theory its phase diagram is calculated using Monte Carlo simulations. Good qualitative agreement is obtained between experiment and theory; better quantitative agreement occurs if the interactions are scaled by a factor of 3/4. A $(\sqrt{3} \times \sqrt{3})^* R30°$ structure at a coverage of 2/3 ML is predicted. © 2002 Elsevier Science B.V. All rights reserved.

1. Introduction

The phase diagram of O/Ru(0 0 0 1) has been determined experimentally by low energy electron diffraction (LEED) up to 0.5 ML [1]. Two different structures have been observed and are well known: A (2×2)-O structure at a coverage of 0.25 ML [2] and a (2×1)-O structure [3] at a coverage of 0.5 ML. Recent scanning tunneling microscopy (STM) and LEED experiments have observed a (2×2)-3O structure at a coverage of 0.75 ML [4–6] and a (1×1)-O at a coverage of 1 ML [7]. The last two structures were predicted by the same density-functional theory (DFT) calculations [8] which are used below for our modeling.

In this system there are two probable binding sites, hcp and fcc, with the hcp-site observed to be favored energetically [2]. Previous modeling of the phase diagram of this system was done via Monte Carlo simulations with the least number of interaction parameters which fitted the experimental phase diagram in a quantitative [1] or qualitative fashion [9]. Piercy et al. modeled this system with both types of binding sites with repulsive interactions only. They were able to explain the observed ratio of the peak order–disorder temperatures at 0.5 ML ($T_{1/2}$) and at 0.25 ML ($T_{1/4}$) by having a spillover onto the fcc sites, $T_{1/2}/T_{1/4} = 0.74$.

However, the absence of attractive interactions does not explain the presence of two regions of coexisting structures observed with STM [10,11]. The first region has both a (2×2)-O structure and a lattice gas [10] and the second the (2×2)-O and (2×1)-O structures [11]. Xiong and Li [9] have calculated the phase diagram from a model with hcp sites only having (an unspecified) first

---

* Corresponding author. Fax: +1-902-494-5191.
E-mail address: mcewenj@is2.dal.ca (J.-S. McEwen).
[1] In the memory of Raphaël Kapfer, Graduate Student of Physics at Cornell University.

Table 1
Interactions energies (eV) to model O/Ru(0 0 0 1)

Site	$E_{site} - E_{hcp}$	V_1	V_2	V_3	V_{lt}	V_{bt}	V_{tt}
hcp	0.0	0.265 (0.23)	0.044 (0.069)	−0.025	−0.039	−0.046	0.058
fcc	0.351 (0.506)	0.158 (0.23)	0.016 (0.069)	0.002	−0.052	−0.044	0.076
fcc–hcp		0.586 (∞)	0.101 (0.069)	0.033			

The interactions of [1] are shown in brackets.

neighbor interaction, V_1, a second neighbor repulsion ($V_2 = 0.1V_1$) and a third neighbor attraction ($V_3 = -0.08V_1$). They obtained both coexistence regions but failed to get the correct ratio of the peak critical temperatures.

In this work we obtain the phase diagram from first principles. Rather than treating the lattice gas interaction energies as fitting parameters we deduce them from DFT calculations of the energies of ordered structures at the above and at other coverages [12]. These interaction energies between the hcp sites, fcc sites and fcc with hcp sites are shown in Table 1. Also included is the calculated binding energy difference of the fcc site with respect to the hcp site. There are significant linear (V_{lt}), bent (V_{bt}) and triangular (V_{tt}) trio interactions, i.e., in addition to the pair interactions V_1, V_2, V_3, for three neighboring O atoms: all lattice structures and symbols are specified in [12]. These trios will destroy the symmetry of the phase diagram around 0.5 ML. The interactions were used successfully to calculate the thermal desorption spectra of O on Ru(0 0 0 1) [12].

The (2×2)-O, (2×1)-O and (2×2)-3O order parameters were calculated for hcp sites and fcc sites separately (see [1]). In addition, to see as in [1] if a honeycomb phase can form with equal occupancy of these sites, we calculated the corresponding order parameter. Also, we calculated the order parameter corresponding to the $(\sqrt{3} \times \sqrt{3})^*R30°$ structure at 2/3 ML [13]. Second order phase transitions were defined at a given chemical potential by the inflection point in the calculated graph of order parameter vs. temperature [1,14]. First order transitions for a given temperature were marked by the discontinuity of the order parameter vs. chemical potential [14,15].

2. Results

Monte Carlo simulations were performed in the grand canonical ensemble (chemical potential specified) using the Metropolis algorithm [16]. Equilibration times of the order of 2^{12} Monte Carlo steps were allowed for each coverage point. Care was taken to initialize the system properly when calculating the regions of coexistence. In addition, for each coverage point we performed an average over at least three independent calculations. To allow adsorption on fcc and hcp sites we used two interpenetrating 60×60 lattices, with periodic boundary conditions. Finite size effects were also examined for the second order transitions up to 0.5 ML for different lattice sizes $L \times L$ ($L = 40, 60, 80$). We used the same scaling law as Piercy et al. for the temperature with the scaling exponent, $v = 2/3$, of the four state Potts model [1]. The coverage was fitted to the form $aL^{-1} + b$, from which we deduced the infinite lattice critical coverage and critical temperature. These values did not change appreciably with respect to the critical values obtained for a 60×60 lattice.

The resulting temperature-coverage phase diagram up to 0.8 ML is shown in Fig. 1a and the corresponding chemical potential-temperature boundaries are shown in Fig. 1b. The upper solid line in Fig. 1a has the same characteristic shape as the phase diagram determined by LEED. We obtain a ratio of the transition temperatures $T_{1/2}/T_{1/4} = 0.83$, close to the experimental and simulated value of Piercy et al. (0.74). However, their simulation required a spillover to the fcc sites as large as 10% at the order–disorder temperature, whereas ours was never greater than 3%. This reduction is mainly due to our larger second neighbor interac-
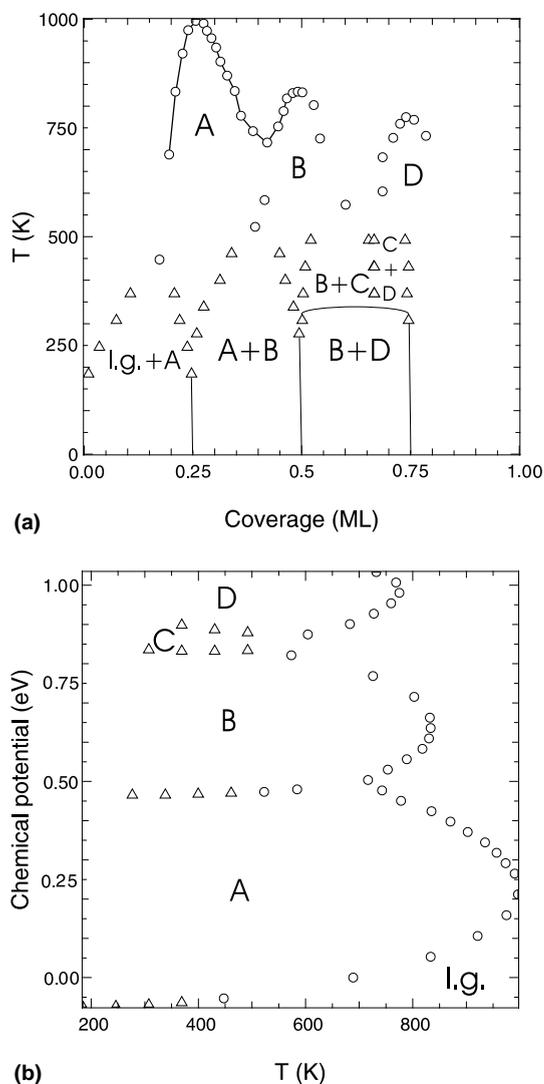
Fig. 1. (a) Phase diagram of O/Ru(0 0 0 1) in the temperature-coverage plane and (b) the chemical potential-temperature plane, with the interactions of Table 1 using the lattice gas model with fcc and hcp sites on interpenetrating 60×60 hexagonal lattices. The triangles indicate first order transitions and the circles second order transitions. The ordered structures are labeled as: (2×2)-O (A), (2×1)-O (B), $(\sqrt{3} \times \sqrt{3})^*R30°$ (C), (2×2)-3O (D), dilute lattice gas (l.g.). A + B denotes the coexistence of structures A and B, etc. The lines in the regions of coexistence indicate the expected low-temperature phase boundaries. Chemical potential is specified with respect to the binding energy of an hcp site.

tion between hcp and fcc sites; and this despite our lower binding difference and first neighbor interaction on fcc sites. In the absence of trios we find

that $T_{1/2}/T_{1/4} \approx 1$. Thus the presence of large trio attractions tends to destroy the (2×1)-O structure at 0.5 ML, thereby decreasing this ratio. This explanation of the ratio, namely hcp trio attractions and little spillover, seems more likely because oxygen is known to occupy hcp-sites at 1 ML [4].

Although we get a reasonable ratio, our prediction of $T_{1/4}$ is too high compared to the observed temperature of 754 K. However, in our calculations the ordinate of Fig. 1a scales with V_1; if we reduce V_1 and all other interactions by a factor of 3/4 we get a very good agreement with experiment. Such a deviation in the interactions could arise if the true adsorption energy of an isolated O atom (the reference energy), is slightly different to that used in the calculations where it was modeled in a 3×3 cell. Due to computational limits larger cells were not tested. We remark that, in another recent DFT calculation for hcp-bonded O/Ru(0 0 0 1) [17], the ratios of interactions to V_1 (there) agree in sign and magnitude within 20%, with the exception of V_{tt}, with those in Table 1. However, V_1 (there) is larger by about 30%, i.e., a rescaling would be necessary, again. The discrepancy between the predicted and experimental upper phase boundary reflects the accuracy of current DFT calculations for adsorbates. Nevertheless, our simulations produce the observed coexistence regions between the lattice gas and the (2×2)-O structure, and the (2×2)-O with the (2×1)-O structure [10,11]. Finally, we find the presence of a $(\sqrt{3} \times \sqrt{3})^*R30°$ structure at 2/3 ML and several coexisting structures above 0.5 ML, labeled B, C, D in Fig. 1. These regions are predictions of our pocket calculation. The $(\sqrt{3} \times \sqrt{3})^*R30°$ structure is favored by the attractive bent trio interaction, V_{bt}. It persists if V_{bt} is reduced, e.g., by 25%, with a corresponding adjustment of other interactions to maintain net energies [12], albeit at a lower temperature. One reason why it has not been observed may be because it exists in a relatively narrow range of temperatures.

3. Conclusions

We have calculated the phase diagram of O/Ru(0 0 0 1) from first principles. In contrast to

previous modeling, we have found that significant occupancy of fcc sites is not necessary to reproduce the features of the high-T region of the phase diagram, including the ratio of transition temperatures at 1/4, 1/2 ML. This is consistent with recent experimental observations. Moreover, the presence of significant hcp trio interactions itself affects this ratio. The interaction parameters obtained from density functional theory must be scaled uniformly by a factor of 3/4 to get excellent agreement with experiment, while preserving structures. We have confirmed the presence of the (2×2)-3O structure and predicted the presence of a $(\sqrt{3} \times \sqrt{3})^{*}R30°$ structure.

Acknowledgements

References

[1] P. Piercy, K. De'Bell, H. Pfnür, Phys. Rev. B 45 (1992) 1869.

[2] M. Lindroos, H. Pfnür, D. Held, D. Menzel, Surf. Sci. 222 (1989) 451.

[3] H. Pfnür, D. Held, M. Lindroos, D. Menzel, Surf. Sci. 220 (1989) 43.

[4] K.L. Kostov, M. Gsell, P. Jakob, T. Moritz, W. Widdra, D. Menzel, Surf. Sci. 394 (1997) L138.

[5] Y.D. Kim, S. Wendt, S. Schwegmann, H. Over, G. Ertl, Surf. Sci. 418 (1998) 267.

[6] M. Gsell, M. Stichler, P. Jakob, D. Menzel, Isr. J. Chem. 38 (1999) 339.

[7] C. Stampfl, S. Schwegmann, H. Over, M. Scheffler, G. Ertl, Phys. Rev. Lett. 77 (1996) 3371.

[8] C. Stampfl, M. Scheffler, Phys. Rev. B 54 (1996) 2868.

[9] G.-M. Xiong, X. Li, Commun. Theor. Phys. 35 (2001) 114.

[10] J. Wintterlin, J. Trost, S. Renisch, R. Schuster, T. Zambelli, G. Ertl, Surf. Sci. 394 (1997) 159.

[11] K. Meinel, H. Wolter, Ch. Ammer, A. Beckmann, H. Neddermeyer, J. Phys. Cond. Matt. 9 (1997) 4611.

[12] C. Stampfl, H.J. Kreuzer, S.H. Payne, H. Pfnür, M. Scheffler, Phys. Rev. Lett. 83 (1999) 2993.

[13] D.P. Landau, Phys. Rev. B 27 (1983) 5604.

[14] O.G. Mouritsen, Computer Studies of Phase Transitions Critical Phenomena, Springer, Berlin, 1984.

[15] D.P. Landau, Phys. Rev. Lett. 28 (1972) 449.

[16] D.P. Landau, K. Binder, A Guide to Monte Carlo Simulations in Statistical Physics, Cambridge University Press, Cambridge, 2000.

[17] A. Eichler, private communication.